A W-Band Electron Nuclear Double Resonance Study of Single Crystals of ^{14}N and ^{15}N Azurin

J. W. A. Coremans,[†] O. G. Poluektov,[†] E. J. J. Groenen,*[,†] G. W. Canters,[‡] H. Nar,[§] and A. Messerschmidt[§]

Contribution from the Centre for the Study of Excited States of Molecules, Huygens Laboratory, Leiden University, P.O. Box 9504, 2300 RA Leiden, The Netherlands, Gorlaeus Laboratories, Leiden Institute of Chemistry, P.O. Box 9502, 2300 RA Leiden, The Netherlands, and Max Planck Institut für Biochemie, Martinsried bei München, Germany

Received June 20, 1996[⊗]

Abstract: We report pulsed Electron-Nuclear-DOuble-Resonance (ENDOR) experiments at 95 GHz and 1.2 K of single crystals of the blue-copper protein azurin and its fully ^{15}N-enriched analogue. The nitrogen ENDOR spectra and their variation with the orientation of the magnetic field with respect to the crystals are described, and it is shown that contributions of five distant nitrogens may be distinguished. For the remote nitrogens of the copper ligands histidines-46 and -117 complete hyperfine and quadrupole tensors are presented and discussed in relation to the structure of the copper site and the extension of the wave function of the unpaired electron. Besides these nuclei three backbone nitrogens show up in the ENDOR spectra, and their hyperfine tensors are reported. One of the backbone nitrogens concerns that of cysteine-112; the others are tentatively assigned to histidine-46 and glycine-45. The wave function of the unpaired electron of oxidized azurin is found to be smeared out over both the copper ligands and parts of the protein backbone.

I. Introduction

Blue-copper proteins have a mononuclear copper center whose electronic structure gives rise to a characteristic intense optical absorption around 600 nm, an almost axial *g*-tensor and a relatively small copper hyperfine splitting in the $g_{||}$ region of the Electron Paramagnetic Resonance (EPR) spectrum.[1,2] Blue-copper proteins are active in the redox-reaction chains in bacteria where they act as electron-transfer proteins. Understanding of the spectral properties of the ligated metal center and of the electron transfer processes requires detailed knowledge of the molecular and electronic structure of the copper site. In recent years a number of X-ray structures of blue-copper proteins have been reported,[3] which reveal a great similarity in the coordination of the copper in the various blue-copper sites. The availability of these crystal structures greatly adds to the effectiveness of spectroscopy in the study of the electronic structure. This is exemplified by the present ENDOR investigation of single crystals of the blue-copper protein azurin.

According to the X-ray diffraction studies of azurin from *Pseudomonas aeruginosa*[4,5] the coordination of the five ligands of the copper ion can be best described as a distorted trigonal bipyramid (Figure 1). Three ligands are at a distance of about 2 Å, the nitrogens (Nδ) of histidine-46 and -117 and the sulfur (Sγ) of cysteine-112. The (NNS) plane spanned by these coordinating atoms almost contains the copper ion. Two other ligands, a sulfur (Sδ) of methionine-121 and an oxygen of glycine-45, occupy the axial positions and interact weakly with copper. In its divalent state the copper ion has one unpaired electron that is delocalized over the copper site.[6] This paramagnetic state can be well studied by EPR. In recent years there has been a trend to go to both lower[7] and higher microwave frequencies than the standard X-band frequency of 9 GHz. The enhanced resolution at higher microwave frequencies has permitted to quantify the small non-axiality of the *g*-tensor.[6,8] The high sensitivity at W-band (microwave frequency of 95 GHz) allows the study of submillimeter single crystals and we have been able to determine the orientation of the principal axes of the *g*-tensor with respect to the copper site.[8]

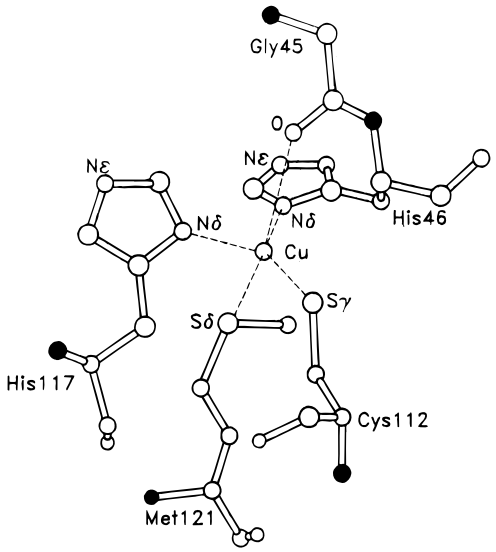

Figure 1. The copper site of azurin from *Pseudomonas aeruginosa*.[5] The backbone nitrogens of the ligands are indicated in black.

[†] Huygens Laboratory, Leiden University.
[‡] Leiden Institute of Chemistry.
[§] Max Planck Institut für Biochemie.
[⊗] Abstract published in *Advance ACS Abstracts,* November 1, 1996.

(1) Adman, E. T. *Adv. Protein Chem.* **1991**, *42*, 145−197.
(2) Sykes, A. G. *Adv. Inorg. Chem.* **1991**, *36*, 377−408.
(3) Adman, E. T. *Curr. Opinion Struc. Biol.* **1991**, *1*, 895−904.
(4) Adman, E. T.; Jensen, L. H. *Isr. J. Chem.* **1981**, *21*, 8−12.
(5) Nar, H.; Messerschmidt, A.; Huber, R.; van de Kamp, M.; Canters, G. W. *J. Mol. Biol.* **1991**, *221*, 765−772.
(6) Penfield, K. W.; Gewirth, A. A.; Solomon, E. I. *J. Am. Chem. Soc.* **1985**, *107*, 4519−4529.
(7) Antholine, W. E.; Hanna, P. M.; McMillin, D. R. *Biophys. J.* **1993**, *64*, 267−272.
(8) Coremans, J. W. A.; Poluektov, O. G.; Groenen, E. J. J.; Canters, G. W.; Nar, H.; Messerschmidt, A. *J. Am. Chem. Soc.* **1994**, *116*, 3097−3101.

S0002-7863(96)02076-8 CCC: $12.00

Hyperfine interactions can be investigated by ENDOR and Electron-Spin-Echo Envelope Modulation (ESEEM) techniques. The coupling of the electron spin with the nuclear spin of the *coordinating* nitrogens of the ligating histidines has been investigated by Q-band (35 GHz) ENDOR experiments on frozen solutions for the blue-copper centers of plastocyanin, azurin, stellacyanin, fungal and tree laccase.[9] The isotropic hyperfine coupling was found to be inequivalent for the two nitrogens, except for plastocyanin, while the anisotropic part of the hyperfine interaction and the quadrupole interaction were not resolved. Unfortunately it remained unclear which isotropic coupling had to be assigned to which nitrogen and this hampered the interpretation of the difference. It has been suggested that the variation of the isotropic hyperfine coupling is related to the deviation of the structure of the copper site from square planar toward tetrahedral.[10]

ESEEM spectroscopy has been successfully applied to a number of metalloproteins.[11] At X-band frequencies (9 GHz) the coupling of the unpaired electron spin with the nuclear spin of the *remote* nitrogens, the nitrogens of the ligating histidines not coordinated to the copper, gives rise to electron-spin-echo envelope modulations. The isotropic hyperfine coupling of the remote nitrogens is on the order of 1 to 2 MHz.[12] Such a value is close to fulfilling the "exact cancellation condition" [13] at X-band frequencies and deep modulations have been observed. The presence of these modulations has been used to establish the ligation of histidine to the copper ion and to estimate the number of ligating histidines in copper proteins.[14] A quantitative analysis of the modulation pattern yields in general information on the quadrupole and hyperfine interaction of the remote nitrogens. The variation found in the quadrupole interaction for different copper proteins has been related to the difference in hydrogen bonding of the remote nitrogens.[15] For the blue-copper sites in stellacyanin and in ascorbate oxidase, the isotropic coupling was found to be different for the two remote nitrogens as observed for the coordinating nitrogens.[16] The anisotropic part of the hyperfine tensor is in almost all studies on frozen solutions taken to be axial. For model compounds containing copper with imidazole as a ligand echo-envelope modulations were studied extensively by various groups.[17−19] The analysis of the modulations did not require inclusion of rhombicity of the hyperfine tensor. In the ESEEM study of Cu(II)-diethylenetriamine-^{15}N-imidazole the rhombicity of the hyperfine tensor was considered and found to be small.[18] The ESEEM studies on single crystals of Cu(II)-doped L-histidine hydrochloride monohydrate and Cu(II)-doped bis(L-histidinato)-cadmium dihydrate allowed an accurate determination of the anisotropic hyperfine tensor.[20,21] In these two cases the anisotropic hyperfine tensors are better described as rhombic and the authors suggested that this should also be the case in copper proteins. Notwithstanding these data, complete hyperfine and quadrupole tensors of histidine nitrogens are not yet available for any blue-copper protein.

In order to fill this gap and to supplement our knowledge of the electronic structure of the copper site of azurin, we have performed elaborate ENDOR experiments on single crystals of azurin and ESEEM experiments on frozen solutions of azurin and azurin mutants. A preliminary report[22] concerned an X-band ESEEM study of azurin and an azurin mutant and ENDOR data in one principal plane of the *g*-tensor for a single crystal of ^{14}N azurin. Here we communicate the full results of the pulsed ENDOR study at 95 GHz of single crystals of ^{14}N azurin and ^{15}N azurin. From the study of ^{14}N azurin we determine the quadrupole tensors of the remote nitrogens of histidine-46 and -117 and assign these tensors to the respective remote nitrogens. Also ENDOR signals have been recorded of a third nitrogen which was detected in an ESEEM study of azurin reported on recently.[22] The quadrupole parameters reveal that this concerns a backbone nitrogen and the directions of the principal axes point to the backbone nitrogen of cysteine-112.

From the study of ^{15}N azurin we determine accurate hyperfine tensors of five nitrogens. Combining the data of the ENDOR studies on ^{14}N and ^{15}N azurin we assign two of the hyperfine tensors to the remote nitrogens of histidine-46 and -117 and a third one to the backbone nitrogen of cysteine-112. The other two nitrogens are weakly coupled to the electron spin and are probably backbone nitrogens as well.

The principal values of the hyperfine tensor of the remote nitrogen of histidine-117 are 1.5 times larger than those of the remote nitrogen of histidine-46. Ab initio calculations indicate that this difference is caused by the different angle between the Sγ-Cu bond and the Cu-Nδ bond for the two histidines leading to a larger delocalization of the electron spin over the histidine-117. The anisotropic hyperfine tensors of the two remote nitrogens are rhombic. Analysis of the anisotropic hyperfine tensor reveals that the most important contributions to the tensor of each remote nitrogen derive from the spin density on Cu, Nδ and Nϵ itself. From the model description, the spin density on the nitrogen atoms of the histidines is obtained as well as an estimate of the spin density on copper.

II. Experimental Section

The isolation and purification of azurin and fully ^{15}N-enriched azurin from *Pseudomonas aeruginosa* has been described elsewhere.[23,24] Single crystals of ^{15}N labeled and unlabeled protein were grown by vapor diffusion.[5] Two different crystal forms, both of space group $P2_12_12_1$ can be obtained. In both crystal forms the unit cell contains sixteen molecules with four molecules per asymmetric unit. The two crystals of the unlabeled protein that we have studied were of the same crystal form with unit cell dimensions $a = 57.8$, $b = 81.0$ and $c = 110.0$ Å. These crystals were kept in mother liquor containing 4.0 M ammonium sulfate, 0.7 M lithium nitrate and 0.1 M acetate at pH 5.5. The crystal of the ^{15}N labeled protein was of the other crystal form with unit cell dimensions $a = 47.8$, $b = 99.2$ and $c = 109.7$ Å. This crystal was also kept at pH 5.5 in a mother liquor of 3.5 M ammonium

(9) Werst, M. M.; Davoust, C. E.; Hoffman, B. M. *J. Am. Chem. Soc.* **1991**, *113*, 1533−1538.
(10) Iwaizumi, M.; Kudo, T.; Kita, S. *Inorg. Chem.* **1986**, *25*, 1546−1550.
(11) Dikanov, S. A.; Tsvetkov, Y. D. *Electron Spin Echo Envelope Modulation (ESEEM) Spectroscopy*; CRC Press: Boca Raton, FL, 1992; pp 316−330.
(12) Jiang, F.; Karlin, K. D.; Peisach, J. *Inorg. Chem.* **1993**, *32*, 2576−2582.
(13) Flanagan, H. L.; Singel, D. J. *J. Chem. Phys.* **1987**, *87*, 5606−5616.
(14) Peisach, J. In *Bioinorganic chemistry of copper*; Karlin, K. D., Tyeklar, Z. Eds.; Chapman & Hall: New York, 1993; pp 21−33.
(15) Jiang, F.; McCracken, J.; Peisach, J. *J. Am. Chem. Soc.* **1990**, *112*, 9035−9044.
(16) Goldfarb, D.; Fauth, J. M.; Farver, O.; Pecht, I. *Appl. Magn. Reson.* **1992**, *3*, 333−351.
(17) Mims, W. B.; Peisach, J. *J. Chem. Phys.* **1978**, *69*, 4921−4930.
(18) Gerfen, G. J.; Singel, D. J. *J. Chem. Phys.* **1994**, *100*, 4127−4137.
(19) Dikanov, S. A.; Spoyalov, A. P.; Hüttermann, J. *J. Chem. Phys.* **1994**, *100*, 7973−7983.
(20) Jiang, F.; Conry, R. R.; Bubacco, L.; Tyeklár, Z.; Jacobson, R. R.; Karlin, K. D.; Peisach, J. *J. Am. Chem. Soc.* **1993**, *115*, 2093−2102.
(21) Colaneri, M. J.; Peisach, J. *J. Am. Chem. Soc.* **1995**, *117*, 6308−6315.
(22) Coremans, J. W. A.; van Gastel, M.; Poluektov, O. G.; Groenen, E. J. J.; den Blaauwen, T.; van Pouderoyen, G.; Canters, G. W.; Nar, H.; Hammann, C.; Messerschmidt, A. *Chem. Phys. Lett.* **1995**, *235*, 202−210.
(23) van de Kamp, M.; Hali, F. C.; Rosato, N.; Finazzi Agro, A.; Canters, G. W. *Biochim. Biophys. Acta* **1990**, *1019*, 283−292.
(24) van de Kamp, M. Ph. D. Thesis, Leiden University, 1993; pp.131−154.

sulfate, 0.7 M lithium nitrate and 0.1 M acetate. All crystals were of submillimeter size, the two unlabeled protein crystals 0.8 × 0.4 × 0.2 mm^3 and 0.8 × 0.4 × 0.3 mm^3 and the labeled one 0.6 × 0.3 × 0.2 mm^3.

The ENDOR experiments were all performed with the homebuilt W-band ESE spectrometer at a microwave frequency of 95 GHz and a temperature of 1.2 K. A detailed description of the pulsed EPR and ENDOR setup is given in ref 25. The crystals were placed in quartz tubes and subsequently mounted into a cylindrical cavity. In the ENDOR experiments a Mims type pulse sequence was used. The separation between the first and the second microwave pulse was typically 350 ns and between the second and the third pulse 210 μs. The width of the radio-frequency pulse, which is applied between the last two microwave pulses, was 200 μs. The repetition rate varied between 40 and 100 Hz.

When the crystals are mounted in the cavity they have an arbitrary orientation with respect to the laboratory frame. The directions of the crystallographic axes (a, b, c) are determined with respect to the laboratory frame through EPR with high accuracy (~2°). In a previous EPR study of a single crystal of azurin from *Pseudomonas aeruginosa* the directions of the principal axes of the *g*-tensor (*x, y, z*) for all sixteen molecules in the unit cell with respect to *a*, *b*, and *c* were established.[8] These data were used to obtain the directions of the principal axes of all 16 *g*-tensors in the laboratory frame for the ENDOR study. Note that in this EPR single-crystal study the EPR data were combined with the X-ray data yielding the orientation of the *x, y,* and *z* axis with respect to the copper site. This means that directions defined with respect to *xyz* can be translated into directions with respect to the copper site and vice versa.

For the crystal of ^{15}N azurin, the crystal form is different from that in the previous single crystal EPR study. Because the orientation of the molecules (and the principal axes systems of the *g*-tensors) with respect to the crystallographic axes is different, a complete single-crystal EPR study on a crystal of ^{15}N azurin had to be performed preceding the ENDOR experiments. The EPR study in combination with simulations of the EPR spectra (as described in ref 8) resulted in accurate directions of the *x, y, z* axes of the sixteen molecules in the unit cell with respect to a, b, c. The ENDOR study is performed with respect to the *x, y, z* axes system of one of the molecules in the unit cell. Consequently the hyperfine tensors that result from the analysis of the ENDOR data are defined in that axes system. Since the X-ray structure is not known for the crystal form of ^{15}N azurin, we do not know the orientation of the *x, y, z* axes system in the copper site for that crystal form. In the discussion of the hyperfine tensors with respect to the copper site we have made the obvious assumption that the orientation of the *x, y, z* axes in the copper site is identical for both crystal forms. Therefore, when the directions of the principal axes of the quadrupole and hyperfine tensors resulting from the ENDOR data of ^{14}N and ^{15}N azurin are discussed with respect to the molecular structure we always refer to the X-ray structure as determined for ^{14}N azurin.[5]

III. Results

A. ^{14}N Azurin. An ENDOR spectrum of the first crystal of ^{14}N azurin is shown in Figure 2b. For this spectrum the direction of the external magnetic field $\vec{B}_0$ was chosen parallel to the *x* axis of one of the molecules in the unit cell, the strength (3.3336 T) so as to be in resonance with the EPR transition of that molecule (cf. Figure 2a). At this magnetic-field setting five ENDOR transitions are observed between 8 and 12 MHz. For a single transition the typical line width is 150 kHz (FWHM). The ENDOR frequencies are symmetrically displaced around the nuclear Zeeman frequency, i.e., 10.26 MHz for a magnetic field of 3.3336 T. For this crystal of ^{14}N azurin ENDOR experiments were performed while the direction of $\vec{B}_0$ was systematically varied in the three principal planes of the *g*-tensor of one molecule and the field strength changed so as to remain in resonance with the corresponding EPR transition.

(25) Disselhorst, J. A. J. M.; van der Meer, H.; Poluektov, O. G.; Schmidt, J. *J. Magn. Reson. A* **1995**, *115*, 183−188.

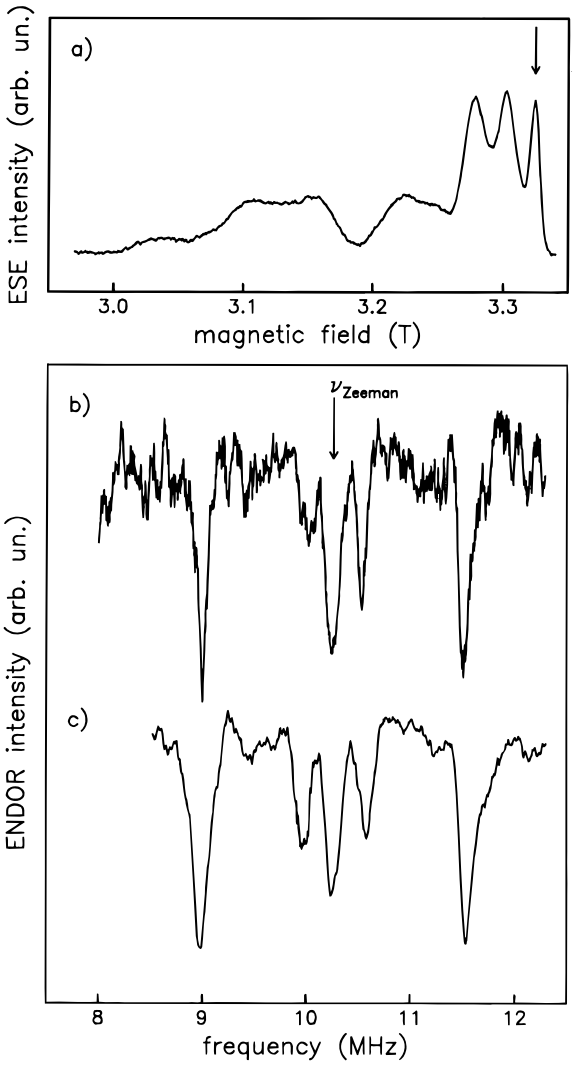

Figure 2. Pulsed EPR (a) and ENDOR (b, c) spectra at 1.2 K of single crystals of azurin from *Pseudomonas aeruginosa*. For all spectra the magnetic field was oriented along the *x* axis of one of the molecules in the unit cell. The field of resonance of that molecule is indicated by the arrow in (a). The pulsed ENDOR spectra between 8 and 12 MHz, taken at that field (3.3336 T), correspond to the first (b) and second (c) single crystal. The ^{14}N nuclear Zeeman frequency at this magnetic field strength is indicated by the arrow in (b).

Only in the *xy* plane was the signal to noise ratio of the ENDOR spectra sufficient to follow the angular dependence of the ENDOR frequencies. The size of the second crystal of ^{14}N azurin was similar to that of the first but owing to improvements in the ENDOR setup well-resolved ENDOR spectra could be obtained also in the *zx* and the *zy* plane of the *g*-tensor. As an illustration of the improvement of the signal to noise ratio compared to that for the first crystal, an ENDOR spectrum of the second crystal is shown in Figure 2c. This spectrum was obtained at the same orientation and strength of $\vec{B}_0$ as the spectrum of the first crystal in Figure 2b. The combination of the measurements on the two single crystals of ^{14}N azurin yielded ENDOR frequencies for all orientations of $\vec{B}_0$ in the *xy* and the *zy* plane and for 60° around the *x* axis in the *zx* plane, as represented in Figure 3. For most directions of $\vec{B}_0$ the spectrum was only measured for frequencies greater than or equal to the nuclear Zeeman frequency. The frequencies below the nuclear Zeeman frequency have the same absolute displacement from the nuclear Zeeman frequency as those above and thus contain no new information. In the *zy* plane additional resonances were found which are indicated in Figure 4a.

B. ^{15}N Azurin. In Figure 5 an ENDOR spectrum of the single crystal of ^{15}N azurin is shown. For this spectrum the direction of $\vec{B}_0$ was in the *xy* plane of the *g*-tensor, rotated 60° from the *x* axis toward the *y* axis. For this orientation eleven ENDOR transitions are observed between 12 and 16 MHz. The ENDOR frequencies are symmetrically displaced around the ^{15}N nuclear Zeeman frequency (14.29 MHz at the field of 3.3099 T). Starting from the high frequency site, the first three ENDOR transitions (1,2,3) are well resolved as are their counterparts below the nuclear Zeeman frequency (1′,2′,3′). Transition 4 is also clearly visible, but its counterpart 4′ appears as a shoulder. For transition 5 the situation is the other way around, transition 5 is weak compared to its counterpart 5′. Transition 6 is found at the ^{15}N nuclear Zeeman frequency. The direction of $\vec{B}_0$ was systematically varied in the principal planes (*xy*, *zx*, *zy*) of the *g*-tensor, and ENDOR spectra were obtained. The frequencies corresponding to transitions 1, 2 and 3 could be followed for all directions of $\vec{B}_0$. This was not the case for the frequencies of transitions 4 and 5 as these transitions were in general weak. Transition 4 was broad as well, causing a larger uncertainty in the determination of the corresponding frequency. Transition 6 was only observed at a few orientations of $\vec{B}_0$. Also for the primed transitions data were obtained in all principal planes. No new information is contained in these data (primed and unprimed transitions are symmetrically displaced around the nuclear Zeeman frequency), but for example the frequency of transition 5′ could be determined more accurately than that of transition 5 for most orientations of $\vec{B}_0$. By combining the primed and unprimed transitions, accurate data sets are obtained for all transitions. All ENDOR frequencies and their variation with the direction of $\vec{B}_0$ in the *g*-tensor principal planes are represented in Figure 6.

IV. Data Analysis

A. Assignment of the ENDOR Spectra of ^{14}N Azurin. The ENDOR frequencies of the crystal of ^{14}N azurin, summarized in Figure 3, can be ascribed to the remote nitrogens of the copper ligating histidines (46 and 117). Based on a comparison with model compounds and other copper proteins, the hyperfine interaction for these nuclei is expected to be on the order of 1 to 2 MHz.[12] This is considerably smaller than the nuclear Zeeman interaction at magnetic field strengths of 3 T and therefore the ENDOR frequencies are symmetrically distributed around the ^{14}N nuclear Zeeman frequency (cf. Figure 2b,c). The spin Hamiltonian describing the unpaired electron spin ($S = {}^1/_2$) and the ^{14}N nuclei ($I = 1$) can be divided in an electronic and a nuclear part as the electron Zeeman term at W-band is much larger than the hyperfine interaction. The nuclear spin Hamiltonian includes a Zeeman, hyperfine and quadrupole interaction term for each nitrogen,

$$H_n = -g(^{14}\mathrm{N})\beta_n \vec{I}\cdot\vec{B}_0 + \langle\vec{S}\rangle\cdot\vec{\vec{A}}\cdot\vec{I} + \vec{I}\cdot\vec{\vec{Q}}\cdot\vec{I}. \qquad (1)$$

Here $g(^{14}\mathrm{N})$ is the nuclear *g*-factor of ^{14}N, β_n the nuclear Bohr magneton, $\langle\vec{S}\rangle$ the expectation value of the electron-spin angular-momentum operator $\vec{S}$, $\vec{\vec{A}}$ the hyperfine tensor and $\vec{\vec{Q}}$ the quadrupole tensor. For each electron spin level two ENDOR transitions are expected for a single ^{14}N nucleus, in total four transitions for each nucleus. The two ENDOR transitions of one electron spin level have the same displacement from the nuclear Zeeman frequency as the two transitions of the other electron spin level but in opposite direction. Therefore all information is contained in half of the ENDOR transitions. Either the ENDOR transitions belonging to one electron spin level or all ENDOR frequencies equal to and above (or below) the nuclear Zeeman frequency can be used in the analysis. The two remote nitrogens are magnetically inequivalent and at most four different transitions may show up at or above the Zeeman frequency. This is indeed observed as can be seen from Figure 3 in which the ^{14}N nuclear Zeeman frequency is indicated by the dashed line. Around 75° in the *zx* plane the four transitions are best resolved (cf. Figure 3). For other directions of $\vec{B}_0$ in the *zx* and the *zy* plane also four transitions are observed, although often two ENDOR transitions become very close in frequency. A broader line then indicates that two transitions are present. For $\vec{B}_0$ along the *x* axis three transitions are observed and apparently two transitions coincide. Indeed, the transition corresponding to the highest frequency for $\vec{B}_0$ parallel to the *x* axis splits into two transitions when $\vec{B}_0$ is turned from the *x* axis toward the $-z$ axis. On the other hand, when $\vec{B}_0$ is turned from the *x* axis toward the *y* axis no splitting is observed.

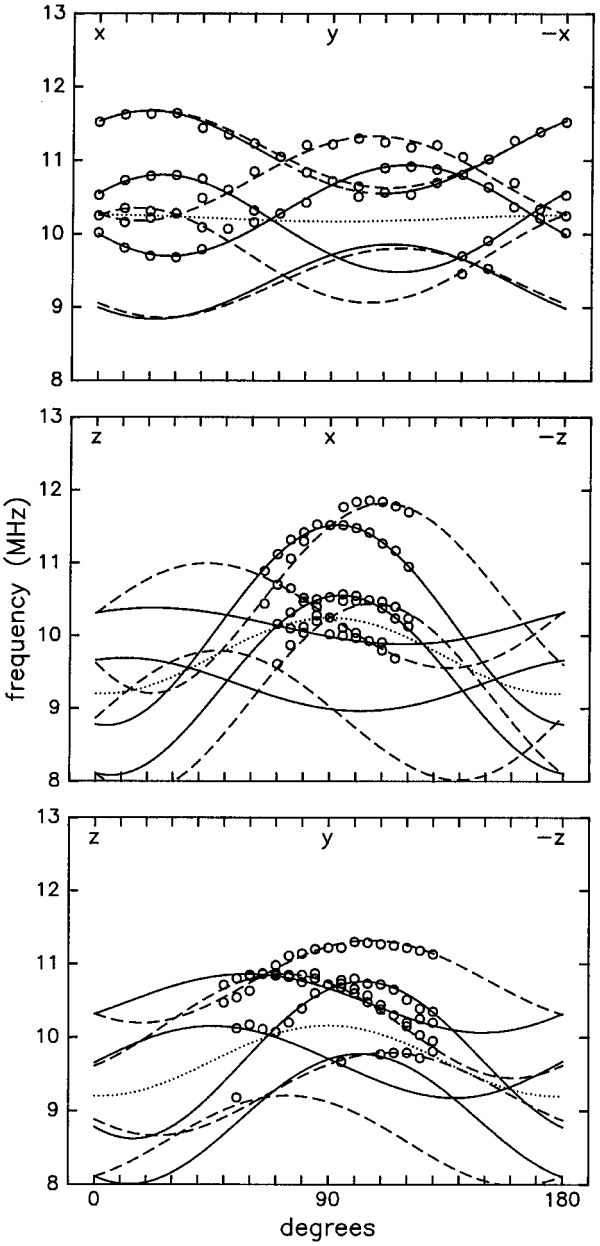

Figure 3. The ^{14}N ENDOR frequencies of the remote nitrogens as a function of the direction of the magnetic field in the *xy*, *zx* and *zy* principal planes of the *g*-tensor. The circles represent the experimental frequencies, the curves represent fits based on eq 1. The solid curves correspond to the remote nitrogen of histidine-46 and the dashed ones to the remote nitrogen of histidine-117. The ^{14}N nuclear Zeeman frequency is indicated by the dotted curve.

Apparently these two transitions coincide within the line width of a single transition in the whole *xy* plane. The variation of the frequencies of the four transitions with the direction of $\vec{B}_0$ is most easily followed in the *xy* and the *zx* plane, but more difficult in the *zy* plane where the transitions are less well separated. The transitions could be followed for 40° on both sides of the *y* axis. When the orientation of $\vec{B}_0$ is close to the *z* or $-z$ axis it is difficult to determine the frequencies of the ENDOR transitions accurately because the ENDOR transitions become broad and weak, and these frequencies are not included in Figure 3. The ENDOR transitions do become weak because at these orientations the EPR lines broaden owing to g-strain and EPR transitions of different molecules in the unit cell overlap (see also ref 8).

The coincidence of two transitions for $\vec{B}_0$ along the *x* axis and even three transitions for $\vec{B}_0$ along the *y* axis complicates the analysis because the connection between the frequency patterns in the different planes is not trivial. To overcome this problem, first only the frequencies in the *xy* plane were analyzed as in this plane the angular variation of the frequencies of the four transitions is best characterized. The frequencies belonging to the same nucleus were analyzed with a non-linear least-squares fit to the Hamiltonian of eq 1. For each remote nitrogen the fit in principle should include eleven parameters. For the quadrupole tensor five parameters are needed, three to define the orientation of the principal axes of the quadrupole tensor x', y', z' with respect to the *g*-tensor principal axes system and two parameters, e^2qQ and η, to represent the principal values as the quadrupole tensor is traceless. By definition

$$e^2qQ = 2Q_{z'z'} \tag{2}$$

and

$$\eta = \frac{Q_{x'x'} - Q_{y'y'}}{Q_{z'z'}} \tag{3}$$

where $Q_{x'x'}$, $Q_{y'y'}$ and $Q_{z'z'}$ correspond to the principal values in order of increasing absolute value. The hyperfine tensor is described by six parameters, three to define the orientation of the hyperfine tensor principal axes x'', y'', z'' with respect to the *g*-tensor principal axes system and three for the principal values $A_{x''x''}$, $A_{y''y''}$ and $A_{z''z''}$. In order to gain preliminary semi-quantitative insight, initially only three parameters a_{iso}, e^2qQ and η were allowed to vary for each nitrogen. The hyperfine interaction was for the moment assumed to be isotropic. The directions of the principal axes of the quadrupole tensor were fixed and taken as found for imidazole and model compounds in quantum-chemical calculations, nuclear-quadrupole resonance and nuclear-magnetic resonance and ESEEM experiments.[26−29] Correspondingly, for each remote nitrogen the directions of the quadrupole principal axes with respect to the imidazole were taken as follows: x' parallel to the N−H bond, z' perpendicular to the imidazole plane and y' perpendicular to x' and z'. A satisfactory fit of the experiment was obtained when the frequencies connected by the solid lines in the top panel of Figure 3 were assigned to the remote nitrogen of histidine-46 and the frequencies connected with the dashed lines to the remote nitrogen of histidine-117. Moreover the quadrupole parameters for both remote nitrogens came out close to those known for the Nϵ of solid imidazole ($|e^2qQ/h| = 1.42$ MHz, $\eta = 0.98$).[30] Subsequently, the values obtained for e^2qQ, η and a_{iso} were used to calculate the ENDOR frequencies of both nitrogens in the *zx* and the *zy* plane and the dependence of the observed ENDOR frequencies on the orientation of the magnetic field in the *zx* and the *zy* plane was reproduced. If the assignment of the ENDOR frequencies to the remote nitrogens in the *xy* plane was reversed, i.e., solid lines assigned to histidine-117 and dashed lines to histidine-46, the agreement between experiment and fit in the *xy* plane was not as good, and the quadrupole parameters came out different from those of solid imidazole. In addition, when the frequencies in the *zx* and the *zy* plane were calculated from the parameters of such a fit the angular dependence of the experimental frequencies in these planes could not be reproduced. Consequently, the frequencies that are connected by the solid and dashed lines have to be assigned to the remote nitrogen of histidine-46 and -117, respectively, and the angular dependence of the frequencies of the four transitions can now be recognized in all three principal planes. This result is based on the distinct orientation of the planes of the imidazoles of the histidines in the copper site and thus of the principal axes of the quadrupole tensors with respect to the principal axes of the *g*-tensor (the angle between the x' axis of the quadrupole tensor of histidine-46 and the x' axis of that of histidine-117 is 22°, between the y' axes 57° and between the z' axes 54°).

At this point an all-parameter fit of the frequencies in the three principal planes is in principle feasible. This would yield complete hyperfine and quadrupole tensors but the much larger anisotropy in the quadrupole tensor than in the hyperfine tensor would inevitably result in large errors in the elements of the hyperfine tensor. The hyperfine tensors can more accurately be determined from the ENDOR data of the crystal of ^{15}N azurin and we postpone the final quantitative analysis of the ENDOR data of ^{14}N azurin until after the analysis of the data of ^{15}N azurin.

The additional ENDOR resonances observed in the *zy* plane, those represented in Figure 4a, do not arise from the remote nitrogens. We assign them to a backbone nitrogen, the same one as was previously recognised in an ESEEM study of azurin.[22] The analysis of these data requires information on the hyperfine interaction of this nucleus that we obtain from the ENDOR study of ^{15}N labeled azurin.

B. Assignment of the ENDOR Spectra of ^{15}N Azurin. For the crystal of ^{15}N azurin, the ENDOR frequencies are determined by the nuclear Zeeman and hyperfine interaction because ^{15}N has nuclear spin $I = {}^1/_2$. The nuclear spin Hamiltonian of eq 1 reduces to

$$H_n = -g(^{15}N)\beta_n \vec{I}\cdot\vec{B}_0 + \langle\vec{S}\rangle\cdot\vec{\vec{A}}\cdot\vec{I} \tag{4}$$

All symbols have the same meaning as in eq 1, and $g(^{15}N)$ is the nuclear *g*-factor of ^{15}N which differs from that of ^{14}N ($g(^{15}N) = -0.5663784$ compared with $g(^{14}N) = 0.4037607$). Both the nuclear Zeeman and the hyperfine interaction scale with the nuclear magnetic moment and for the crystal of ^{15}N azurin the hyperfine interaction of the remote nitrogens will be smaller than the Zeeman interaction like for the crystal of ^{14}N azurin. Again the ENDOR frequencies will be symmetrically displaced around the nuclear Zeeman frequency. For the crystal of ^{15}N azurin, one ENDOR transition is expected for each electron spin level, two transitions per nucleus. Those nitrogens observed for the crystal of ^{14}N azurin, the two remote nitrogens of the

(26) Palmer, M. H. *Chem. Phys.* **1987**, *115*, 207−218.
(27) Garcia, M. L. S.; Smith, J. A. S.; Bavin, P. M. G.; Ganellin, C. R. *J. Chem. Soc., Perkin Trans. 2* **1983**, 1391−1399.
(28) McDowell, C. A.; Naito, A.; Sastry, D. L.; Takegoshi, K. *J. Magn. Reson.* **1986**, *69*, 283−292.
(29) Colaneri, M. J.; Peisach, J. *J. Am. Chem. Soc.* **1992**, *114*, 5335−5341.
(30) Hunt, M. J.; MacKay, A. L.; Edmonds, D. T. *Chem. Phys. Lett.* **1975**, *34*, 473−475.

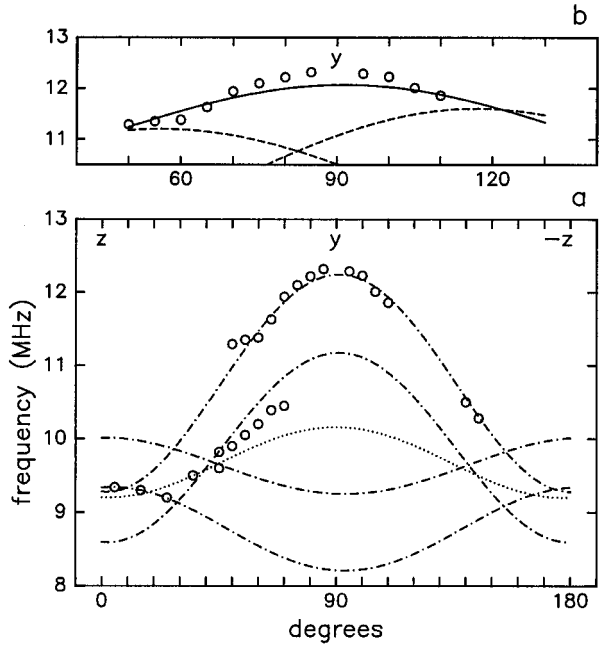

Figure 4. The ^{14}N ENDOR frequencies of the backbone nitrogen as a function of the direction of the magnetic field in the *zy* plane. The circles represent the experimental frequencies. (a) The results of the fits based on eq 1 in which the directions of the principal axes were varied are represented by the dashed dotted curves. The ^{14}N nuclear Zeeman frequency is indicated by the dotted curve. (b) Enlarged representation of the highest experimental ENDOR frequencies in the region 40° to 140° in the *zy* plane. The results of the fits based on eq 1 in which the direction of the *z*′ axis was fixed either perpendicular to the C−N−C fragment of histidine-46, dashed curve, or perpendicular to the C−N−C fragment of cysteine-112, solid curve.

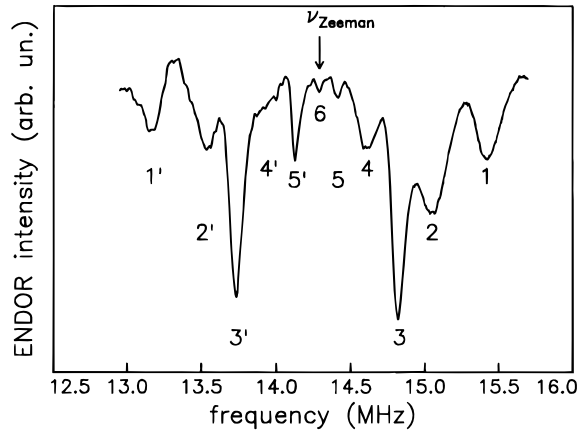

Figure 5. The pulsed ENDOR spectrum at 1.2 K between 13 and 16 MHz of a single crystal of fully ^{15}N-enriched azurin from *Pseudomonas aeruginosa*. The direction of the magnetic field was 60° in the *xy* plane of one of the molecules in the unit cell. The magnitude of the magnetic field was 3.3099 T so as to be in resonance with the EPR transition of that molecule. The ENDOR transitions corresponding to nucleus 1 are indicated by 1 and 1′, etc. The ENDOR transition indicated by 6 coincides with the ^{15}N nuclear Zeeman frequency at this magnetic field strength, which is indicated by the arrow.

histidines and the backbone nitrogen, give rise to (at most) six transitions in the ^{15}N ENDOR spectrum of the crystal of ^{15}N azurin while eleven transitions have been observed (cf. Figure 5).

The transition at the Zeeman frequency (transition 6) corresponds to so-called matrix nitrogens that have virtually no coupling to the electron spin. Owing to the loss of sensitivity in the pulsed ENDOR experiment at the Zeeman frequency, this transition is greatly reduced in intensity compared with the

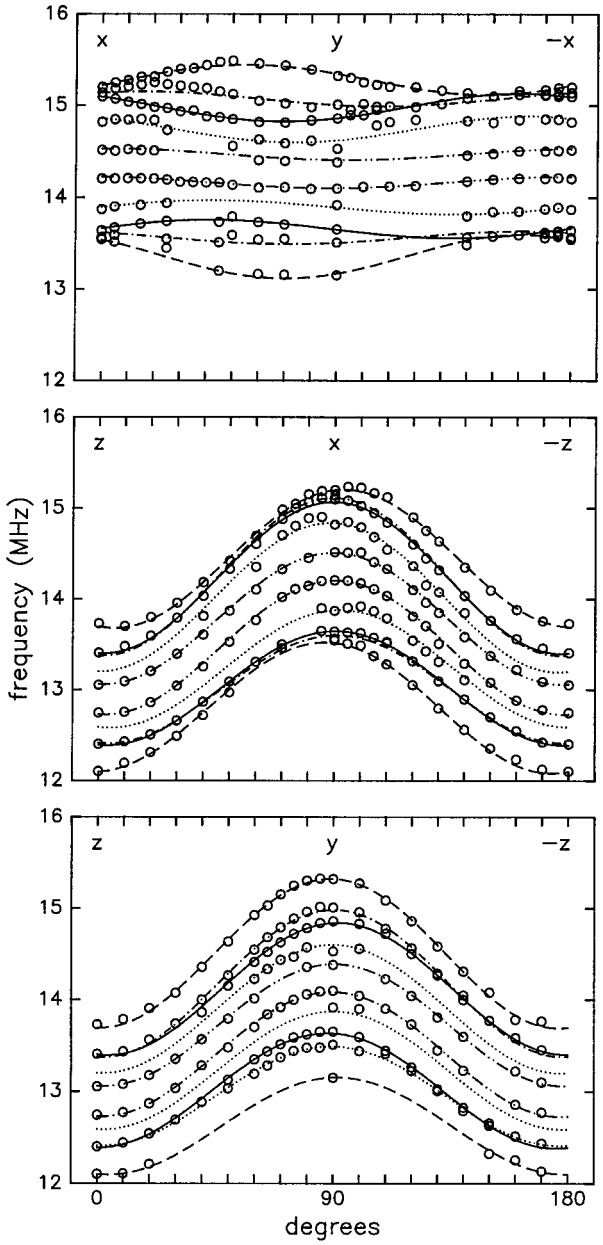

Figure 6. The ^{15}N ENDOR frequencies corresponding to the five nitrogens as a function of the direction of the magnetic field in the *xy*, *zx* and *zy* planes. The circles represent the experimental frequencies; the curves represent fits based on eq 4. As regards the curves: the dashed lines correspond to nucleus 1 (the remote nitrogen of histidine-117), the dash-dotted lines to nucleus 2 (the backbone nitrogen of cysteine-112), the solid lines to nucleus 3 (the remote nitrogen of histidine-46), the dotted lines to nucleus 4 and the dash-dot-dot lines to nucleus 5.

others which facilitates the detection of the weakly coupled nitrogens. The other ten transitions arise from five nuclei (transition 1 and 1′ belong to nucleus 1, 2 and 2′ to nucleus 2, up to 5 and 5′ to nucleus 5). The ENDOR frequencies of these five nuclei are indicated in Figure 6 as a function of the orientation of $\vec{B}_0$ in the three principal planes of the *g*-tensor. A considerable anisotropy exists in the *zx* and the *zy* plane. The variation of the ENDOR frequencies is mainly caused by the change in nuclear Zeeman frequency from 12.90 MHz at the *z* axis to 14.38 MHz at the *x* axis and to 14.26 MHz at the *y* axis, which completely overshadows the anisotropy of the hyperfine interaction in the *zx* and the *zy* plane. In first approximation the hyperfine interaction (divided by 2) at a given orientation can be obtained by calculating the displacement of the observed

ENDOR frequency from the nuclear Zeeman frequency at that orientation. The result for the transitions above the Zeeman frequency, labeled 1 to 5 in Figure 5, is shown in Figure 7 and a clear variation of the hyperfine interaction in the principal planes of the *g*-tensor is observed for the different nuclei. When this procedure is repeated for transitions 1′ to 5′, the angular dependence is about identical (except for the sign) and therefore not shown. The angular dependence of the frequencies belonging to nuclei 1, 2 and 3 can be followed in the three principal planes. The frequency of nucleus 1 is at all orientations of $\vec{B}_0$ the highest and clearly separated from the frequencies of the other nuclei except near the *x* axis where the frequencies of nuclei 1, 2 and 3 overlap. The frequencies of nucleus 2 show up separated from those of the other nuclei in the regions 40°−90° in the *xy* plane and 50°−100° in the *zy* plane, while they coincide with the ones of nucleus 3 for all orientations of $\vec{B}_0$ in the *zx* plane. The frequencies of nuclei 1 and 2 are very close in the region 5°−35° in the *xy* plane and a broadened ENDOR line is observed. The angular dependence of the frequencies of nucleus 4 is not as well defined as that of the other nuclei. The lines are in general weak and broad which limits the accuracy with which the ENDOR frequencies could be determined. The ENDOR frequency of nucleus 5 is always nearest to the nuclear Zeeman frequency and varies hardly with the orientation of $\vec{B}_0$ in any of the principal planes.

The next step is to identify which of the five nuclei correspond to the remote nitrogens of histidine-46 and -117. The hyperfine interaction of the remote nitrogens at each orientation of $\vec{B}_0$ can be obtained from the ^{14}N ENDOR data by calculating the average displacement from the nuclear Zeeman energy of the two frequencies belonging to the same electron spin level for each nucleus. This gives to good approximation half of the hyperfine interaction. After multiplication with the ratio of the nuclear magnetic moments ($|g(^{15}N)|/|g(^{14}N)|$), these data have been compared with the ^{15}N data of Figure 7. In this way nucleus 1 is found to correspond to the remote nitrogen of histidine-117 and nucleus 3 to that of histidine-46. Nucleus 2 we ascribe to the backbone nitrogen which was observed previously in an ESEEM study of azurin.[22] Comparison of the ^{14}N and ^{15}N hyperfine data reveals that the angular dependence of the hyperfine interaction is best defined in the ENDOR study of ^{15}N azurin.

C. Hyperfine Interaction Tensors from ^{15}N ENDOR. The hyperfine tensors of the various nitrogens can be obtained by fits of the ^{15}N ENDOR frequencies to the Hamiltonian of eq 4. For each nucleus the six parameters of the hyperfine tensor were varied. The frequencies of the ENDOR transitions of both electron spin levels were included in the fits, i.e., those of the primed and unprimed transitions (e.g. 5 and 5′ for nucleus 5). To obtain reliable hyperfine tensors, a proper description of the nuclear Zeeman interaction is necessary as this interaction is the dominant contribution to the ENDOR frequencies. Therefore the nuclear Zeeman interaction was included in the analysis of the ENDOR frequencies by taking the microwave frequency (or, equivalently, the magnitude of $\vec{B}_0$) as a parameter. This was done for all five nuclei separately and yielded an average microwave frequency of 95.05 GHz for a $g(^{15}N)$ value of −0.56638.[31] Inclusion of the microwave frequency as a parameter is important in view of the fact that different values have been reported for the nuclear *g*-factor (e.g. $g(^{15}N) = -0.56591$ in ref 32). Although the difference may seem small, such a variation may cause a difference in the principal values of the hyperfine tensors of 50 kHz when the microwave frequency is kept fixed. The hyperfine tensors of the five nuclei that result from the fits are presented in Table 1, while the calculated frequencies are represented in Figures 6 and 7. The averaged microwave frequency of 95.05 GHz was used. As can be seen from Figures 6 and 7 the observed and calculated frequencies agree well for the remote nitrogens, the backbone nitrogen and nucleus 5. Correspondence is of course less for nucleus 4 as the experimental data are not so well defined in this case. Although for the backbone nitrogen the calculated frequencies deviate from the experimental ones in the region 0°−35° in the *xy* plane, the calculated ones are still within the line width of the broad ENDOR lines observed in this region. The uncertainty around the *x* axis leads to a slightly larger inaccuracy in the principal values and directions of the principal axes for this nucleus compared to those for the remote nitrogens (8°, 0.08 MHz versus 5°, 0.05 MHz). The uncertainty in the principal values of the hyperfine tensor for nucleus 5 is even

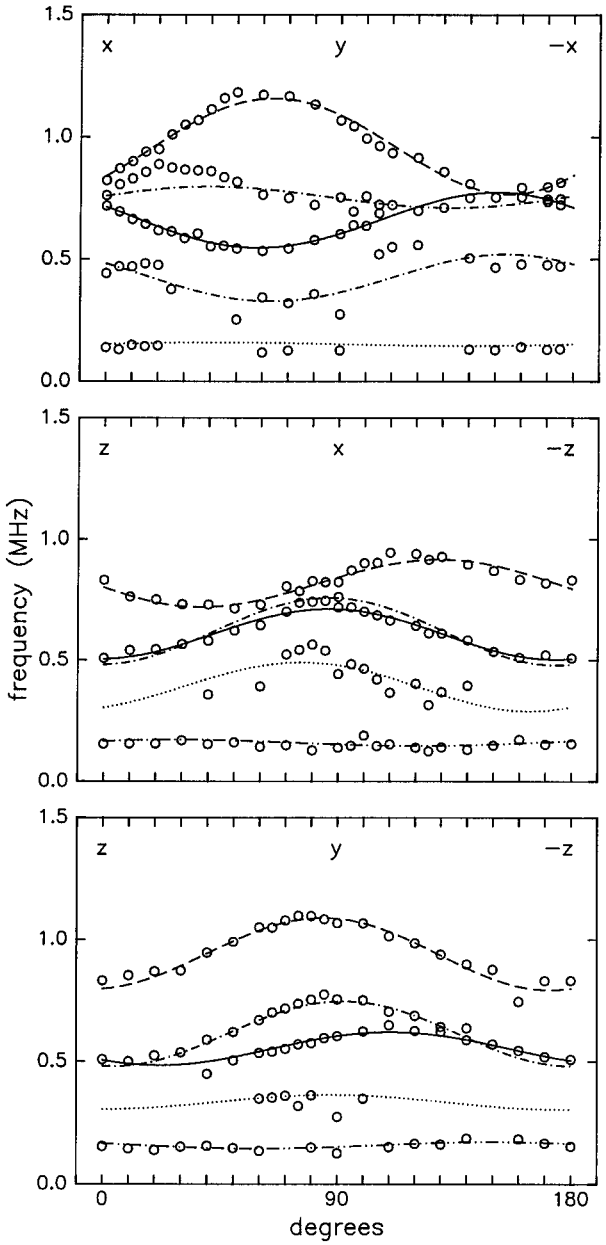

Figure 7. The ^{15}N ENDOR frequencies corrected for the ^{15}N nuclear Zeeman contribution of the nitrogens 1 to 5 as a function of the direction of the magnetic field in the *xy*, *zx* and *zy* planes. The circles represent the experimental frequencies, the curves represent fits based on eq 4 which are also corrected for the ^{15}N nuclear Zeeman contribution. Curve symbols as in Figure 6.

(31) Bruker EPR/ENDOR Frequency Table.
(32) Bruker NMR NQR Periodic Table.

Table 1. Hyperfine Tensors for the Five Nitrogens as Determined from the ^{15}N ENDOR Study: The Isotropic Hyperfine Coupling (in MHz), the Principal Values (in MHz) and the Direction Cosines of the Principal Axes System $x''y''z''$ in the xyz Axes System of the g-Tensor[a]

	a_{iso}/h	$A_{x''x''}/h$	$A_{y''y''}/h$	$A_{z''z''}/h$		x	y	z
Nϵ histidine-117	1.30	1.65	1.26	0.98	x''	−0.440	−0.897	0.040
					y''	0.577	−0.316	−0.753
					z''	0.689	−0.308	0.657
Nϵ histidine-46	0.87	1.10	0.80	0.69	x''	0.843	−0.523	0.131
					y''	−0.520	−0.726	0.449
					z''	−0.140	−0.447	−0.884
N backbone (cysteine-112)	0.95	1.14	1.02	0.68	x''	0.754	0.657	0.020
					y''	−0.653	0.752	−0.085
					z''	−0.071	0.051	0.996
N 4	0.55	0.75	0.48	0.41	x''	0.890	−0.415	0.191
					y''	0.286	0.832	0.475
					z''	−0.356	−0.368	0.859
N 5	0.22	0.25	0.23	0.19	x''	0.323	−0.357	0.876
					y''	0.723	0.690	0.015
					z''	−0.610	0.629	0.482

[a] The isotropic hyperfine couplings and the principal values of the hyperfine tensors as obtained from experiment have been multiplied by the absolute value of $g_n(^{14}N)/g_n(^{15}N)$ and therefore refer to ^{14}N. The sign of the isotropic hyperfine coupling has been taken positive. Typical errors in the principal values and the orientations of the principal axes amount to 0.05 MHz and 5° for the Nϵ of histidine-117 and the Nϵ of histidine-46, 0.08 MHz and 8° for the backbone nitrogen, 0.15 MHz and 20° for nitrogen four, and 0.02 MHz and 20° for nitrogen five.

Table 2. Quadrupole Tensors of the Nϵ's of Histidine-46 and −117 and of the Backbone Nitrogen of Cysteine-112: Quadrupole Parameters e^2qQ/h (in MHz) and η and the Principal Values (in MHz) and the Direction Cosines of the Principal Axes System $x'y'z'$ in the xyz Axes System of the g-Tensor[a]

	e^2qQ/h	η	$Q_{x'x'}/h$	$Q_{y'y'}/h$	$Q_{z'z'}/h$		x	y	z
Nϵ histidine-117	−1.43	0.95	0.02	0.70	−0.72	x'	−0.145	−0.867	−0.476
						y'	0.887	0.099	−0.452
						z'	0.439	−0.488	0.755
Nϵ histidine-46	−1.37	0.86	0.05	0.64	−0.68	x'	0.482	−0.798	0.362
						y'	0.014	−0.407	−0.914
						z'	0.876	0.446	−0.185
N backbone (cysteine-112)	−3.10[b]	0.40[b]	0.47[b]	1.09[b]	−1.55[b]	x'	0.558	0.291	0.777
						y'	0.262	0.980	0.168
						z'	0.788	0.110	0.606

[a] The sign of e^2qQ was chosen negative. Typical errors in the principal values and the orientations of the principal axes for the remote nitrogens are 0.04 MHz and 2°. For the backbone nitrogen the absolute values of the direction cosines of the principal axes system $x'y'z'$ are given (see text). [b] The quadrupole parameters and principal values of the quadrupole tensor were taken from the ESEEM study. The simulations have been optimized resulting in values slightly different from those reported previously.[22]

smaller (0.02 MHz). On the other hand, the anisotropy for nucleus 5 is on the order of the experimental accuracy and therefore not too much weight can be attributed to the orientation of the principal axes as found.

Comparison of the anisotropy of the hyperfine tensors (defined as $(|A_{x''x''}| - |A_{z''z''}|)/|a_{iso}|$, with $A_{x''x''}$ the absolute largest hyperfine element and $A_{z''z''}$ the absolute smallest), reveals 25% anisotropy for nucleus 5 and 50% for the remote and backbone nitrogens. For nucleus 4 the anisotropy is estimated to be even 60%. The larger anisotropy may well be the reason that the ENDOR lines for this nucleus are broad compared to those for the other nuclei. A similar observation has been made in the ENDOR study of ^{14}N azurin, where the quadrupole tensor of the backbone nitrogen is found to be more anisotropic than those of the remote nitrogens, resulting in significantly broader ENDOR lines for the backbone nitrogen than for the remote nitrogens of the ligating histidines. Narrow ENDOR transitions were observed for nucleus 5 in the study of ^{15}N azurin and also for protons with small hyperfine couplings (data not shown). In general there seems to be a correspondence between the width of the ENDOR line and the anisotropy of the interaction. In analogy to the broadening of the EPR transitions owing to g-strain we refer to this as quadrupole and hyperfine strain.

D. Quadrupole Interaction Tensors from ^{14}N ENDOR. The quadrupole tensors of the remote nitrogens can be obtained from the ^{14}N data from fits of the ENDOR frequencies to the nuclear spin Hamiltonian of eq 1. The hyperfine tensors from the study of ^{15}N azurin have been used in this analysis of ^{14}N azurin, after correction for the difference in the nuclear g-values. The five parameters of the quadrupole tensor have been varied and all the frequencies in Figure 3 have been taken into account in the calculations. Calculated and experimental frequencies agree well as can be seen from Figure 3 where the calculated frequencies for the remote nitrogen of histidines-46 and -117 are represented by solid and dashed lines, respectively. The quadrupole tensors of both remote nitrogens are presented in Table 2. The orientation of the principal axes of the quadrupole tensors deviates only slightly from the axes system as defined in section IVA. The quadrupole parameters e^2qQ and η are similar for both remote nitrogens. Neither inclusion in the fits of additional frequencies from measurements around the z axis in the zy plane (data not shown), nor inclusion of the elements of the hyperfine tensor as variables in the fit significantly affected the result for the quadrupole tensor, i.e., variations were limited to less than 2° in the directions of the principal axes and less than 50 kHz in the principal values.

For the backbone nitrogen, ENDOR data were measured in the zy plane. In the analysis the directions of the principal axes of the quadrupole tensor were varied while the principal values were kept fixed. The hyperfine parameters were taken from the ^{15}N ENDOR study and the parameters for the principal values of the quadrupole tensor from the ESEEM study (cf. Tables 1 and 2). As Figure 4a shows, a satisfactory fit of the ENDOR frequencies is obtained. The quadrupole tensor is represented in Table 2. The signs of the Q_{xy} and Q_{zx} elements relative to those of the other elements could not be determined.

As a consequence only the absolute values of the direction cosines describing the orientation of the $x'y'z'$ axes system in the xyz axes system are given.

V. Discussion

The 95 GHz pulsed ENDOR study of single crystals of ^{14}N and ^{15}N azurin has provided quantitative data concerning the hyperfine and quadrupole interaction of several nitrogen nuclei in the vicinity of the copper center: the remote nitrogens of the copper ligating histidines-46 and -117 and three more nitrogens that are weakly coupled to the unpaired electron. The discussion of these data is divided into two parts. First we consider the quadrupole and then the hyperfine interaction.

A. Quadrupole Interaction. Complete quadrupole tensors have been obtained for the remote nitrogens of the ligating histidines. The principal values of the quadrupole tensors of these nitrogens are nearly equal with differences of at most 60 kHz. The values of e^2qQ/h and η are indicative for nitrogens forming relatively strong hydrogen bonds.[15] In the solid state the orientation of the principal axes of the nitrogen quadrupole tensor with respect to imidazole does not show much variation from one molecule to another. This concerns both histidines and imidazoles in various model compounds.[21,28,29,33] One axis is perpendicular to the molecular plane, one axis parallel to the N−H bond and one in the imidazole plane perpendicular to the other two directions. From the ENDOR data of the remote nitrogens the orientation of the principal axes has been determined with high accuracy (± 1°) and, as shown in section IV A, this has been used to assign the hyperfine and quadrupole tensors of the remote nitrogens to histidine-46 and to histidine-117. For both remote nitrogens one axis is found almost perpendicular to the plane of the imidazole. The angle between the normal of the imidazole plane and this axis is 5° and 6° for histidine-46 and -117, respectively. Another axis is almost parallel to the N−H bond in both cases, the difference being 5° for histidine-46 and 6° for histidine-117. The deviations are small and within the combined error margins of the X-ray (±2°), EPR (±2°) and ENDOR data (±1°) and we will neglect these deviations in the rest of the discussion.

For the remote nitrogen of histidine-117 the z' axis, associated with the largest absolute principal value, is perpendicular to the imidazole plane and the y' axis, associated with the principal value of intermediate magnitude, is in the plane of the imidazole perpendicular to the N−H bond. For the remote nitrogen of histidine-46 it is the other way round (see Figure 8). If in the analysis of the ENDOR frequencies of histidine-46 the z' axis was forced to be perpendicular to the molecular plane, the agreement between experiment and calculation was slightly worse and this difference between the two remote nitrogens may be significant. It is interesting to note that Garcia et al[27] predicted that the directions associated with the largest and the intermediate principal values will interchange if the absolute value of e^2qQ/h becomes less than 1.35 MHz, which is very close to the value found for histidine-46 (see Table 2). There have been examples that the interchange of the axes is not that sharply defined as predicted by Garcia.[28,29] In imidazolium hydrogen maleate the z' and the y' axis have interchanged with respect to the situation in solid imidazole.[26] The authors explained the interchange of the axes by a small reduction of 0.045 e in the π-electron occupancy of the nitrogen in the case of imidazolium hydrogen maleate. It has been proposed that the differences in the π-electron occupancy are determined by the strength of the hydrogen bond.[15,34] For azurin this would mean that the remote nitrogen of histidine-46 forms a slightly less strong hydrogen bond than the remote nitrogen of histidine-117.[15] X-ray and NMR data reveal that the remote nitrogens are involved in relatively strong hydrogen bonds with different acceptors, water for histidine-117 and the carbonyl oxygen of asparagine-10 for histidine-46.[5,35]

We ascribe the additional ENDOR transitions in the zy plane (Figure 4a) to a backbone nitrogen based on the corresponding quadrupole parameters $e^2qQ/h = -3.10$ MHz and $\eta = 0.40$. These values are very similar to the quadrupole parameters observed for nitrogens in backbone-like configurations, e.g. $e^2qQ/h = -3.030$ MHz, $\eta = 0.412$ for the amide nitrogen in glycylglycine,[36] and $e^2qQ/h = -3.350$ MHz, $\eta = 0.385$ for the amide nitrogen of the central glycine in triglycine,[37] where the sign is inferred from calculations. We observed this nitrogen in an X-band ESEEM study of azurin,[22] and at that time we concluded that this backbone nitrogen might belong to either histidine-46, as this nitrogen is next to the glycine-45 carbonyl bond, or to cysteine-112, as the cysteine sulfur is known to carry an appreciable spin density.[6] Later this nitrogen was also recognised in 2D HYSCORE experiments,[38] and, based on a comparison with ascorbate oxidase, suggested to correspond to the backbone nitrogen of histidine-46.

As seen above for the remote nitrogens, the orientation of the principal axes of the quadrupole tensor may be useful in assigning a quadrupole and hyperfine tensor to a specific nitrogen. The direction of the principal axes of the quadrupole tensor of a backbone nitrogen has not been determined experimentally, but obtained from ab initio SCF calculations. Rabbani et al. have calculated the electric field gradient for the nitrogen atoms in di- and triglycine using a Dunning double-ζ basis.[37] For the amide nitrogens the z' axis was found perpendicular to the C−N−C fragment of the peptide chain and the other two axes were calculated to be in the C−N−C plane with the x' axis not parallel to the N−H bond but rotated 30° from this bond toward the N-Cα bond. We obtained similar results from ab initio SCF calculations on a small backbone fragment ($HCO\text{-}NH_2\text{-}CH_3$) with the GAMESS-UK[39] program. The coordinates of the atoms were directly taken from the X-ray structure of azurin, i.e., the backbone structure of the residues glycine-45 and histidine-46. The electric field gradient at the nitrogen nucleus was calculated using different basis sets (6-311G**, double-ζ including polarisation functions and triple ζ including polarisation functions). In all calculations the z' axis was found perpendicular to the C−N−C fragment. The calculated value of e^2qQ varied from −3.4 to −3.8 MHz, which corresponds reasonably well to the experimental value. For an extended backbone fragment like $NH_2\text{-}CH_2\text{-}CO\text{-}NH_2\text{-}CH_2\text{-}HCO$ the z' principal axis of the amide nitrogen remained perpendicular to the C−N−C fragment. The results for the other two principal values and axes were less clear cut, depending strongly on the chosen basis set and on the length of the N−H bond. Using the double-ζ basis, we varied this bond length between 0.85 and 1.2 Å. For bonds shorter than 1 Å, the x' axis was

(33) Colaneri, M. J.; Potenza, J. A.; Schugar, H. J.; Peisach, J. *J. Am. Chem. Soc.* **1990**, *112*, 9451−9458.

(34) Ashby, C. I. H.; Cheng, C. P.; Brown, T. L. *J. Am. Chem. Soc.* **1978**, *100*, 6057−6063.

(35) van de Kamp, M.; Canters, G. W.; Wijmenga, S. S.; Lommen, A.; Hilbers, C. W.; Nar, H.; Messerschmidt, A.; Huber, M. *Biochemistry* **1992**, *31*, 10194−10207.

(36) Palmer, M. H. *Z. Naturforsch.* **1984**, *39a*, 1108−1111.

(37) Rabbani, S. R.; Edmonds, D. T.; Gosling, P. *J. Magn. Reson.* **1987**, *72*, 230−237.

(38) Kofman, V.; Farver, O.; Pecht, I.; Goldfarb, D. *J. Am. Chem. Soc.* **1996**, *118*, 1201−1206.

(39) Guest, M. F.; Fantucci, P.; Harrison, R. J.; Kendrick, J.; van Lenthe, J. H.; Schoeffel, K.; Sherwood, P. *GAMESS-UK User's Guide and Reference Manual*; Computing for Science (CFS) Ltd. Daresbury Laboratory, 1993.

calculated closest to the N−H bond; for longer ones the y' axis was closest. Values of η between 0.05 and 0.32 were found and these low values of η reflect the problem in the calculations : the quadrupole tensors are not too far from axial and small differences in the structure or basis sets give rise to large differences in the orientations of these axes.

From these calculations and those of Rabbani et al. we conclude that the quadrupole z' axis of a backbone nitrogen is perpendicular to the C−N−C fragment. This finding has been used to identify the backbone nitrogen. We have performed two additional fits of the ENDOR frequencies in the *zy* plane that belong to the backbone nitrogen (see Figure 4a), in which we kept the z' axis fixed either perpendicular to the C−N−C fragment of histidine-46 or to that of cysteine-112. The directions of the other two principal axes of the quadrupole tensor were left free. The result, represented in Figure 4b, reveals that the experimental data are only reproduced for z' perpendicular to the backbone fragment of cysteine-112. Consequently, the nitrogen that gives rise to the additional frequencies in the *zy* plane, and which was also observed in ESEEM experiments at X-band frequency,[22] corresponds to the backbone nitrogen of cysteine-112.

B. Hyperfine Interaction. Hyperfine tensors have been determined for five nitrogen nuclei around copper. We first discuss the remote nitrogens of histidines-46 and -117. The isotropic hyperfine interaction will be considered and subsequently the anisotropic part of the hyperfine interaction in relation to the spin-density distribution over the copper site. Finally we briefly touch upon the hyperfine tensors of the other three nitrogens.

The isotropic hyperfine interaction of the remote nitrogen of histidine-117 is approximately 1.5 times larger than that of histidine-46 (Table 1). Previously differences have been observed between the isotropic hyperfine couplings of the copper-coordinated nitrogens of ligating histidines in a number of blue-copper proteins.[9] For azurin values of 17 and 27 MHz have been determined, again a ratio of about 1.5,[9] but it remained unclear which of these hyperfine couplings belongs to histidine-46 and which to histidine-117. Our result for the remote nitrogens renders it plausible to assign the largest coupling to the copper-bound nitrogen of histidine-117 and the smallest one to that of histidine-46. This inference is corroborated by a 95 GHz ESEEM study of the coordinated nitrogens.[40] The ratio of the isotropic hyperfine coupling of the coordinated and the remote nitrogens then becomes approximately twenty for both histidines. This would imply a different total spin density on the two histidines while the distribution of the spin density within the two histidines would be comparable. This conclusion is nicely supported by preliminary ab initio SCF calculations on a truncated copper site of azurin that we performed with the GAMESS-UK[39] program. The site consisted of copper surrounded by two imidazoles representing the histidines and an SCH_3^- fragment representing the cysteine. In total 125 electrons were described by 182 basis functions. Although the calculations have the common SCF flaw to localise the unpaired electron[41] (in our case on the cysteine sulfur), interesting information on the electron spin distribution within the histidine rings is obtained. A spin-density analysis of the wave function of the unpaired electron shows that for both histidines (actually imidazoles) the ratio between the spin densities for the coordinated and remote nitrogens is about twenty while the spin density on the histidine-117 is calculated 1.5 times larger than that on histidine-46.

What is the origin of the unequal distribution of the unpaired electron over both histidine ligands? The X-ray structure of azurin has revealed three differences as regards the binding of the two histidines to copper. First, the distance of the coordinated nitrogens to the copper may be different (2.00 Å and 2.07 Å for histidine-117 and −46, respectively, according to X-ray diffraction). Secondly, the rotation of the imidazole plane around the Cu-Nδ bond with respect to the NNS plane is larger for histidine-117 than for histidine-46. The size of this tilt is reflected by the angle between the normal to the imidazole plane and the *z* axis (the principal axis of the *g*-tensor perpendicular to the NNS plane) which is 23° for histidine-46 and 39° for histidine-117. Thirdly, the angle between the Sγ-Cu and Cu-Nδ bond is different (131° and 121° for histidine-46 and -117, respectively). When in the SCF calculations the distance of the coordinated nitrogens to the copper was taken equal almost no change in the distributions of the spin density was observed. If the angle between the Sγ-Cu bond and the Cu-Nδ bond for histidine-46 was made identical to that for histidine-117 the spin density on both histidines became about equal while the ratio between the spin density on the coordinated nitrogen and on the remote nitrogen remained 20 for both histidines. The calculations show that the copper d_{xy} orbital has predominantly σ overlap with the Nδ lone pair orbital of the histidines, in agreement with the result of SCF-Xα-Scattered Wave calculations on a model of C_S symmetry of the blue-copper site of plastocyanin.[42] (Note that the nomenclature of the orbitals on copper and the cysteine-112 sulfur refers to the following axis system: z perpendicular to the NNS plane, and the x and y axes in this plane with x parallel to the Cu-Sγ bond. This axes system should not be confused with the *g*-tensor principal axes system.) This overlap is insensitive to the tilt of the histidine but varies with the orientation of the Cu-Nδ bond with respect to the Sγ-Cu bond in the NNS plane, as in azurin the Nδ lone pair orbitals of both histidines are almost in the plane containing the copper d_{xy} orbital. Apparently the orientation of the Cu-Nδ bond of the histidine-117 in the NNS plane is such that it leads to a larger spin density on that histidine than on histidine-46.

The anisotropic hyperfine tensors of both remote nitrogens are rhombic with principal values 0.23, −0.06, −0.17 MHz for the remote nitrogen of histidine-46 and 0.35, −0.04, −0.31 MHz for that of histidine-117. For both anisotropic hyperfine tensors the value of $A_{y''y''}$ is almost zero, and the absolute values of $A_{x''x''}$ and $A_{z''z''}$ are approximately a factor 1.5 larger for the remote nitrogen of histidine-117. The directions of the principal axes of the anisotropic hyperfine tensors of both remote nitrogens are similar when looked upon in the respective local axes systems x', y', z' as defined for the quadrupole tensors in section IV A (see Figure 8). The z'' axes, associated with the smallest principal values, are almost perpendicular to the imidazoles. The angle between z'' and z', the direction perpendicular to the molecular plane, is 5° for histidine-46 and 14° for histidine-117. The x'' axes, associated with the largest principal value, are almost in the molecular planes and rotated from the Nϵ-H bond, x', toward the Nϵ-Cδ bond by 25° and 35° for histidine-46 and -117. For both remote nitrogens this axis is almost parallel to the Cu-Nϵ direction (the angle between x'' and the Cu-Nϵ vector is 6° for histidine-46 and 9° for histidine-117). The directions of the principal axes are comparable to those of remote nitrogens of model compounds as obtained from single crystal ESEEM studies.[20,21]

(40) Coremans, J. W. A.; Poluektov, O. G.; Groenen, E. J. J.; Canters, G. W.; Nar, H.; Messerschmidt, A. to be published.

(41) Larsson, S.; Broo, A.; Sjölin, L. *J. Phys. Chem.* **1995**, *99*, 4860−4865.

(42) Guckert, J. A.; Lowery, M. D.; Solomon, E. I. *J. Am. Chem. Soc.* **1995**, *117*, 2817−2844.

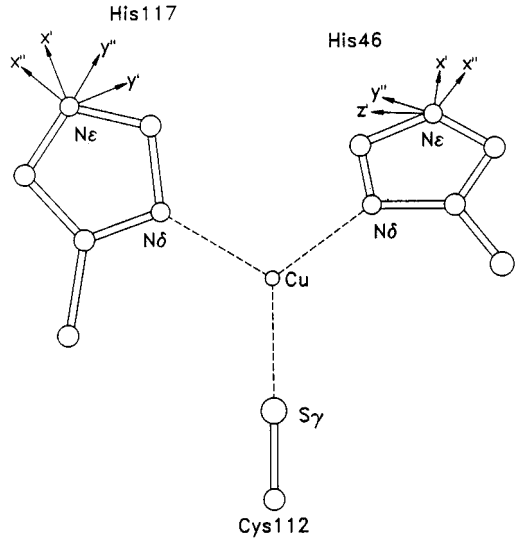

Figure 8. The experimentally determined orientations of the principal axes of the quadrupole tensors ($x'y'z'$) and of the hyperfine tensors ($x''y''z''$) of the remote nitrogens of the ligating histidines in the copper site of azurin. For clarity, the axes almost perpendicular to the plane of the histidines, i.e., the y' and z'' axes for histidine-46 and the z' and z'' axes for histidine-117, have been omitted. For both remote nitrogens the x' axis is almost parallel to the Nϵ-H bond and the x'' axis parallel to the Cu-Nϵ vector.

To gain insight into the electron-spin distribution in the copper site a simple model of the anisotropic hyperfine tensor is constructed. The anisotropic hyperfine tensor may be written as a sum of the contributions of electron-spin densities ρ_i in atomic orbitals $|\varphi_i\rangle$:

$$\frac{\vec{\vec{A}}_{\text{aniso}}}{h} = g(^{14}\text{N})\beta_n g_e \beta_e \sum_i \rho_i \left\langle \varphi_i \left| \frac{3\hat{r}\hat{r} - \vec{\vec{E}}}{r^3} \right| \varphi_i \right\rangle \qquad (5)$$

Here $\vec{\vec{E}}$ is the unit matrix, $\vec{r}$ is the position of the electron spin with respect to the nucleus and $\hat{r} = \vec{r}/|\vec{r}|$. Although in principle spin density distributed over the whole copper site should be taken into account in order to describe the anisotropic hyperfine tensor of one remote nitrogen we only consider contributions of the spin density on four atoms. Besides the remote nitrogen itself, the coordinated nitrogen of the same histidine, the copper and the sulfur of cysteine-112. The anisotropic hyperfine tensor is proportional to the spin density ρ and inversely proportional to r^3. The copper and sulfur are rather far away from the remote nitrogen (~4 and 6 Å, respectively) but do carry the bulk of the spin density.[6] As far as the histidine is concerned our SCF calculations indicate that only the Nδ carries an appreciable amount of spin density. Of course spin density on the remote nitrogen itself has to be considered because even a small amount of spin density on that atom gives an appreciable contribution to the anisotropic hyperfine interaction.

As mentioned, the interaction between the copper ion and the histidine consists of a σ overlap of the d_{xy} orbital with the lone pair orbital of the Nδ. Consequently, we model the spin density on the Nϵ and Nδ atoms as distributed over sp^2 hybrid atomic orbitals. For the copper and sulfur atoms the spin densities are assigned to respectively a d_{xy} and a p_y orbital because these orbitals appear to determine almost the complete electron-spin distribution on these two atoms.[6] For the one-center contribution to the anisotropic hyperfine interaction (i.e., the interaction of the remote nitrogen Nϵ with the electron-spin density on this atom), the integral in eq 5 has been evaluated explicitly[43] by expressing the sp^2 hybrid orbitals as combinations of 2s and 2p Slater orbitals with an effective nuclear charge Z of 4.35.[44] In order to calculate the two-center contributions, the electron-spin density distribution on the other atoms has been replaced by point spins.[45] For the Nδ the spin density in the sp^2 hybrids has been replaced by three point spins of equal magnitude, in the directions of the three hybrid orbitals at a distance of 0.68 Å from the nucleus. The spin density in the sulfur p_y orbital is represented by two point spins at a distance of $\pm$1.02 Å from the sulfur nucleus along the p_y-axis. The spin density in the copper d_{xy} orbital is represented by four point spins at a distance of 0.38 Å along the four lobes of this orbital. The distances of 0.68, 1.02 and 0.38 Å correspond with the average distance with respect to the nucleus of an electron in a Slater 2s or 2p orbital for nitrogen ($Z = 4.35$), a 3s or 3p orbital for sulfur ($Z = 5.45$) and a 3d orbital for doubly ionised copper ($Z = 14.60$).

The calculated anisotropic hyperfine tensor is not very sensitive to the precise distribution of the point spins around the copper and sulfur nuclei or to the distance of the point spin to the nuclei. For instance, when the contribution to the anisotropic hyperfine tensor of a remote nitrogen was calculated of a spin density of one on either copper or sulfur and the point spins were distributed so that a copper $d_{x^2-y^2}$ orbital was represented instead of a d_{xy} or the distances of the point spins to the nuclei were varied $\pm$ 0.2 Å, the variation in the anisotropic hyperfine elements was less than 5 kHz which is small compared to the experimental uncertainty of 50 kHz.

In the actual calculations of the anisotropic hyperfine tensors of the remote nitrogens according to the model outlined above, we consider the spin densities as parameters. First we took only spin density on the copper atom into account, an assumption used in many simulations of X-band ESEEM spectra of copper-imidazole complexes.[12,16,18,19] In a linear least-squares fit the experimental anisotropic hyperfine tensor was already reproduced rather well, especially for the remote nitrogen of histidine-46, albeit for an unphysical spin density much larger than one on copper. Even when spin density on the remote nitrogen itself was included in the analysis the spin density calculated on copper remained larger than one. Spin density on the Nδ had to be considered in order to arrive at an acceptable spin density on copper. The contribution of the cysteine sulfur to the anisotropic hyperfine tensor turned out to be fairly small. In the final analysis we nevertheless included the sulfur and required the sum of the spin density on this atom and on copper to be one. Furthermore we know, as discussed above, that the ratio between the spin density on the Nδ and the Nϵ is for both histidines approximately 20, which was used as a further constraint in the analysis. The spin densities for which the best agreement between calculated and experimental anisotropic hyperfine tensors for both remote nitrogens is obtained are presented in Table 3. The deviation of the calculated from the experimental values is for all elements within the experimental uncertainty of 50 kHz, except for the $z'y'$ element of histidine-117.

In Table 3 also the separate contributions of the spin densities on the different atoms to the anisotropic hyperfine tensors are given in the local axes systems $x'y'z'$ of the remote nitrogens. The contributions of the different spin densities on Nϵ, Nδ and Cu are equally important and that of the spin density on the

(43) Groenen, E. J. J.; Buma, W. J.; Schmidt, J. *Isr. J. Chem.* **1989**, *29*, 99−108.
(44) Singel, D. J.; van der Poel, W. A. J. A.; Schmidt, J.; van der Waals, J. H.; de Beer, R. *J. Chem. Phys.* **1984**, *81*, 5453
(45) Kemple, M. D. In *Multiple Electron Resonance Spectroscopy*; Dorio, M. M., Freed, J. H. Eds.; Plenum Press: New York, 1979; pp 409−436.

Table 3. Anisotropic Hyperfine Tensors (in MHz) of the Remote Nitrogens of Histidine-46 (Top) and Histidine-117 (Bottom) in Their Local Axes Systems $x'y'z'$ as Defined in Section IVA[a]

histidine-46

	exp			calc		
	x'	y'	z'	x'	y'	z'
x'	0.186	−0.118	0.003	0.173	−0.103	0.004
y'	−0.118	−0.012	−0.013	−0.103	0.007	−0.001
z'	0.003	−0.013	−0.174	0.004	−0.001	−0.180

	Cu d_{xy} 0.6 ± 0.2			S p_y (0.4)			Nδ sp^2 0.049 ± 0.006			Nϵ sp^2 0.0024 ± 0.0003		
ϱ	x'	y'	z'	x'	y'	z'	x'	y'	z'	x'	y'	z'
x'	0.062	−0.062	0.002	0.018	−0.007	0.003	0.052	−0.034	0.000	0.043	0.000	0.000
y'	−0.062	−0.013	−0.001	−0.007	−0.008	−0.001	−0.034	−0.015	0.000	0.000	0.043	0.000
z'	0.002	−0.001	−0.049	0.003	−0.001	−0.010	0.000	0.000	−0.037	0.000	0.000	−0.086

histidine-117

	exp			calc		
	x'	y'	z'	x'	y'	z'
x'	0.230	−0.172	0.072	0.265	−0.144	0.015
y'	−0.172	0.063	−0.107	−0.144	0.032	−0.005
z'	0.072	−0.107	−0.293	0.015	−0.005	−0.297

	Cu d_{xy} 0.6 ± 0.2			S p_y (0.4)			Nδ sp^2 0.094 ± 0.018			Nϵ sp^2 0.0047 ± 0.0009		
ϱ	x'	y'	z'	x'	y'	z'	x'	y'	z'	x'	y'	z'
x'	0.064	−0.066	0.004	0.019	−0.009	0.011	0.099	−0.069	0.000	0.083	0.000	0.000
y'	−0.066	−0.013	−0.002	−0.009	−0.010	−0.003	−0.069	−0.028	0.000	0.000	0.083	0.000
z'	0.004	−0.002	−0.051	0.011	−0.003	−0.009	0.000	0.000	−0.071	0.000	0.000	−0.166

[a] For both nitrogens the top left tensor represents the experimental (cf. Table 1) and the top right one the calculated tensor. This last tensor is the sum of contributions of the spin density on copper, on the sulfur of cysteine-112, on the coordinated and on the remote nitrogen itself. The separate contributions and the magnitude of the spin densities ϱ are given. Note that the spin density on the sulfur atom could not be determined from this study but was related to the spin density on copper (see text). The error margins of the spin densities on the nitrogens indicate the possible variations of these densities within the model.

cysteine S is small. From Table 3 the main features of the anisotropic hyperfine tensor can be understood, i.e., the rotation of the x'' axis in the plane of the imidazole away from the Nϵ-H bond and the non-axiality of the tensor. The rotation of the x'' axis, which is determined by the $x'y'$ element, stems from the spin densities on the Cu and the Nδ. Both these contributions rotate the x'' axis in the same direction. This rotation is the same for both remote nitrogens because of the identical orientation of the Cu-Nϵ and Nδ-Nϵ vectors in the local $x'y'z'$ axes systems. These vectors are within the accuracy of the X-ray structure in the plane of the imidazoles and for both remote nitrogens make identical angles with the x' axis, 30° for the Cu-Nϵ and 20° for the Nδ-Nϵ vector. (Notice that the anisotropic hyperfine interaction arising from a single point spin is axial and that the axis associated with the largest principal value is along the vector connecting the point spin and the nucleus.) The contribution of each atom to the anisotropic hyperfine tensor is virtually axial. For the Cu and the Nδ the largest principal value is positive and the corresponding axis in the plane of the imidazole and for the Nϵ the largest principal value is negative and the corresponding axis perpendicular to the plane. The combination explains the rhombicity of the overall tensor. From this we may infer that the modeling of the spin density on the remote nitrogen by sp^2 hybrid orbitals is appropriate. We conclude that a model of the anisotropic hyperfine tensors of the remote nitrogens of both histidines has to take into account the contributions of spin density on Cu, Nδ and Nϵ.

For histidine-117 the agreement between the experimental and calculated anisotropic hyperfine tensor of the remote nitrogen is somewhat less than for histidine-46. This especially concerns the discrepancy between the calculated $z'y'$ matrix element and the experimental one (cf. Table 3), in other words the rotation of the z'' axis away from the normal to the imidazole plane. Such a rotation goes not only beyond the simple model but is difficult to explain as such, and it might not be real. X-ray data indicate slight differences in the geometry of the copper sites of the four molecules in the asymmetric unit. The ENDOR measurements have been performed on one of the molecules in the unit cell and it may well be that for that molecule the orientation of the histidine-117 deviates slightly. Unfortunately this hypothesis can not be tested because the ^{15}N ENDOR study was performed on a crystal form for which the X-ray structure has not been determined. A rotation of about 5°, probably insignificant in terms of X-ray resolution, would be sufficient to bring the deviation between experiment and calculations within the experimental error. A somewhat larger rotation so that z'' becomes parallel to z' would make the agreement between the calculated and experimental anisotropic hyperfine tensor of the remote nitrogen almost as good for histidine-117 as for histidine-46. This shows how sensitive the anisotropic hyperfine tensor is to the orientation of the histidine in the copper site.

As mentioned before, spin density on the cysteine Sγ hardly contributes to the anisotropic hyperfine tensor of the remote nitrogens. Even for unit spin density on the Sγ the largest contribution to an element of the anisotropic hyperfine tensor would be only 50 kHz. Consequently the spin density on the cysteine Sγ can not be determined from this study. We find a spin density of 60% ± 20% on copper. This is a reasonable result compared to the 41% d_{xy} character of the ground state wave function derived from X-ray absorption studies of plastocyanin[46] and the 42% to 54% from SCF-Xα-SW calculations on a model site for plastocyanin.[6,42] In these calculations the

spin densities on the coordinated nitrogens were determined to be 5%, a value that is also derived from the isotropic hyperfine coupling by Werst et al.[9] For azurin we estimated the spin density on the coordinated nitrogen of histidine-46 to be 4.9% (cf. Table 3), similar to the results for plastocyanin. The spin densities on the remote nitrogens are well defined within the present model, the uncertainty being less than 1‰. From the spin density in the sp^2 hybrid orbitals on the Nδ and Nϵ atoms the isotropic hyperfine constant has been calculated from the 2s character of these hybrids using a value of 1062 MHz for unit spin density in a 2s orbital on nitrogen.[47] This gives for histidine-46 for the remote nitrogen 0.86 MHz and for the coordinated nitrogen 17.2 MHz, for histidine-117 values of 1.67 and 33.3 MHz, respectively. For histidine-46 the agreement with the experimental values of 0.87 and 17 MHz is perfect which underscores the applicability of the model. (Note that in contrast to π radicals the isotropic hyperfine interaction does not result from polarisation effects but directly from spin density in the hybrid orbitals on the remote nitrogens that also contribute to the anisotropic hyperfine interaction.) For histidine-117 with experimental values of 1.30 and 27 MHz the agreement is less good. However, as mentioned, the deviation between calculated and experimental anisotropic hyperfine tensor became smaller when z'' was taken parallel to z'. For this geometry the calculated isotropic hyperfine interaction becomes 1.41 MHz for the remote and 28.2 MHz for the coordinated nitrogen, i.e., also the isotropic hyperfine interaction becomes better described. This strengthens the idea that the actual orientation of the histidine-117 for the azurin molecule in the asymmetric unit that we have investigated with ENDOR may be somewhat different from that of the average copper site given in the X-ray diffraction study.

The anisotropic hyperfine tensors of the remote nitrogens of azurin are sensitive probes of the spin-density distribution over copper and the histidines, as essentially covered by our model. For the d_{z^2} ground-state complex Cu(II)-doped L-histidine hydrochloride monohydrate a simple picture in which only point spins were considered was found adequate in the description of the anisotropic hyperfine tensor of the remote nitrogen.[29] However a similar approach was not successful for the $d_{x^2-y^2}$ ground state complex a Cu(II)-doped bis(1,2-dimethylimidazole) dichloride.[33]

The isotropic hyperfine interaction for the backbone nitrogen of cysteine-112 is slightly larger than that of the remote nitrogen of histidine-46 (cf. Table 1), in line with the result of an X-band ESEEM study.[22] The high resolution of pulsed ENDOR at W-band is demonstrated by the observation of the fourth and fifth nitrogen in the ENDOR study of ^{15}N azurin. For these nitrogens quadrupole interaction data are unfortunately not available which makes assignment of the tensors to specific nitrogens impossible. A candidate for the fourth nucleus is the backbone nitrogen of histidine-46. This nitrogen is next to the carbonyl bond of glycine-45. The distances from this nitrogen to the copper and sulfur are 4.1 and 4.4 Å respectively. The relatively short distance to the atoms that carry most of the spin density might explain the relatively large anisotropy in the hyperfine interaction observed for this nitrogen. For the fifth nitrogen the anisotropic character of the hyperfine interaction is small, which points to a distance of this nitrogen from the copper of at least 5 Å. Possible candidates are the backbone nitrogen of glycine-45 and that of histidine-117 with distances to the copper of 5.5 and 5.7 Å, respectively. The results of an NMR study of cobalt(II)-substituted azurin may be taken as support for the assignment to the backbone nitrogen of glycine-45 because the amide proton of glycine-45 was found to be isotropically shifted.[48] Unfortunately no detailed NMR data are available for copper(II) azurin at the moment. The delocalization of the electron spin over the backbone is intriguing and requires future investigation.

VI. Conclusion

The pulsed ENDOR study at 95 GHz of single crystals of azurin and ^{15}N azurin has enabled a detailed probing of various nitrogens in the surrounding of the copper center. First, the remote nitrogens of the ligating histidines-46 and -117. Complete hyperfine and quadrupole tensors have been determined, assigned to the respective remote nitrogens and analyzed. The principal values of the hyperfine tensor of the remote nitrogen for histidine-117 are 1.5 times larger than those for histidine-46. Quantum-chemical calculations indicate that this difference is related to the difference in the angle between the Sγ-Cu and Cu-Nδ bonds for the two histidines. The relevant contributions to the anisotropic hyperfine tensors derive from the spin densities on Cu, Nδ and Nϵ itself. The spin density on Nϵ is found to be 0.0024 for histidine-46 and 0.0047 for histidine-117. Secondly, the backbone nitrogen that was previously recognised in an ESEEM study on azurin. From the orientation of the principal axes of the quadrupole tensor of this nucleus it is concluded that this backbone nitrogen belongs to cysteine-112. The principal values of the hyperfine tensor of this nitrogen are found to be in between those of the Nϵ's of histidine-46 and histidine-117. Thirdly, two more nitrogens have been detected with significantly smaller hyperfine interactions. Probably these concern backbone nitrogens as well and we tentatively assign the tensors to the backbone nitrogens of histidine-46 and of glycine-45 or histidine-117.

The present study confirms that high-frequency ENDOR provides the opportunity to study individual nuclei in great detail. The unpaired electron of oxidised azurin is found to be smeared out over the copper ligands and the wave function extends over parts of the protein backbone as well. High-field pulsed ENDOR turns out to be the method of choice to study the weakly bound nitrogen nuclei. Recently we have observed deep electron-spin-echo envelope modulations arising from the interaction of the electron spin with the coordinating Nδ's of the ligating histidines. The analysis of these is underway and promises to provide detailed data for these nitrogens as well.

Acknowledgment. We gratefully acknowledge Dr. M. C. van Hemert for his assistance in the quantum-chemical calculations and Dr. M. van de Kamp for the preparation of the ^{15}N labeled protein. This work has been performed under the auspices of the Biomac Research School of Leiden and Delft Universities and was supported by the Netherlands Foundation for Chemical Research (SON) with financial aid from the Netherlands Organisation for Scientific Research (NWO).

JA962076U

(46) George, S. J.; Lowery, M. D.; Solomon, E. I.; Cramer, S. P. *J. Am. Chem. Soc.* **1993**, *115*, 2968−2969.

(47) Pople, J. A.; Beveridge, D. L. *Approximate Molecular Orbital Theory*; McGraw Hill: New York, 1970; pp 128−135.

(48) Moratal, J.; Salgado, J.; Donaire, A.; Jiménez, H. R.; Castells, J. *Inorg. Chem.* **1993**, *32*, 3587−3588.